Journal of Molecular Liquids 340 (2021) 117302

Contents lists available at ScienceDirect

Journal of Molecular Liquids

journal homepage: www.elsevier.com/locate/molliq

Polyimide-free vertical alignment in a binary mixture consisting of nematic liquid crystal and reactive mesogen: Pretilt modulation via two-step polymerization

Young Jin Lim [a], Jun Hyeok Lee [a], Gwan Yong Lee [a], Mira Jo [a], Eun Ji Kim [a], Tae Hyung Kim [a], MinSu Kim [a,*], Myong-Hoon Lee [b], Seung Hee Lee [a,*]

[a] Department of Nano Convergence Engineering and Department of Polymer Nano Science and Technology, Jeonbuk National University, Jeonju, Jeonbuk 54896, Korea
[b] The Graduate School of Flexible and Printable Electronics, Jeonbuk National University, Jeonju, Jeonbuk 54896, Korea

ARTICLE INFO

Article history:
Received 14 June 2021
Revised 8 August 2021
Accepted 15 August 2021
Available online 18 August 2021

Keywords:
Polyimide-free alignment
Pretilt control
Liquid crystal
Reactive mesogen
Vertical alignment
Polymer-stabilized vertical alignment

ABSTRACT

The alignment and order control in an anisotropic system is of interest in broad fields of research and engineering. Although the alignment control technique has been developed for decades in commercialization of liquid crystal (LC) displays, achieving polyimide-free high homogeneity in LC alignment and precise modulation of pretilt remain challenging. Here, we demonstrate a LC-reactive mesogen (RM) binary mixture that can control vertical alignment with neither alignment-inducing additives nor polyimides coated on the surface. A synthesized RM itself plays both roles of a vertical alignment inducer and pretilt fixer. To achieve it, we conduct two-step polymerization. In step 1, UV exposure energy is controlled minimal enough to polymerize RMs partially as LC is well aligned vertically. In step 2, a voltage is applied from patterned electrodes to produce pretilt and then second UV is exposed to fix the pretilt by polymerization of the residual RMs. The result contributes to aiding the efficiency of the material synthesis, fabrication process and enhance electro-optic properties like quicker response time, low-threshold, operating voltage, and on-state transmittance. We believe this approach will open a new way to achieve the pretilt in anisotropic medium from not only engineering but also scientific perspectives.

1. Introduction

Over the decades, displays have been a crucial element for gaining, consuming, or exchanging information. In liquid crystal displays, one of the widespread inventions to control light into expressing meaningful information, the molecular anisotropy and its ordering control are the key to achieve the best electro-optic performance of display devices. Based on how the ground state of liquid crystals (LCs) is set and how to reorient them, each display company has developed its own display mode. In the vertical alignment (VA) mode among those various LC display modes, to achieve high performances, like short response time and wide field-of-view, the alignment of the VA mode has been controlled to be set in multi-domains [1–3]. Such development conveys polymer sustain alignment (PSA) or polymer-stabilized (PS) VA mode [4–6]which is one of the flagship modes in TV sets. In PS-VA mode, the initial LC director has an approximately 89-degree pretilt angle into different azimuthal directions for a ready-to-reorient status. The PS-VA mode requires to mix LCs with negative dielectric anisotropy with polymerizable reactive mesogen (RM) in LC mixtures.

Since the beginning of development in display modes, polyimide containing hydrophobic side chains is the most familiar material to generate robust vertical alignment [7]. However, coating of the polyimide requires multiple fabrication steps, including thermal process at above 250 °C, with thickness of less than 100 nm, which result in inefficiency in cost and time for fabrication [8,9]. Moreover, the high-temperature fabrication process is not suitable for flexible substrates. Engineers in this industrial field have long been looking for an alternate method or materials that can eliminate such complex fabrication steps. For example, some reports proposed LC-polymer composites whose internal structure shows nanosize-confined LCs in polymer matrix or network and exhibits electro-optical switching between optically isotropic and induced anisotropic states [10–13]. Such LC-polymer composites have not commercialized yet. However, eliminating the polyimide-coating process has been ongoing on the vertical [14] and planar alignments [15,16].

For the polyimide-free vertical alignment, additives like nanoparticles and monomers to LC mixtures have been reported

* Corresponding authors.
E-mail addresses: minsu.kim@jbnu.ac.kr (M. Kim), lsh1@jbnu.ac.kr (S.H. Lee).

https://doi.org/10.1016/j.molliq.2021.117302
0167-7322/

[17–20]. Among those, the PS-VA mode shows relatively successful trajectory on the commercialization. In recent work on this mode, two or more additives are mixed with a host LC. For example, on the one hand, Inoue et al. and Li et al. reported RMs that contain two or more methyl methacrylate-functional groups at two ends to control vertical alignment by polymerization of RMs at the surface [21,22]. On the other hand, Son et al. reported two additives to induce vertical alignment and fix it: hydroxyl-functionalized LCs and acrylic monomer. The hydroxyl-functional group is for hydrogen bonding between the end of molecules and surface. And benzene rings and alkyl chains help the molecules stand up and mix with LCs [23]. The acrylic-functional group is to polymer-stabilize the pretilt by being exposed to UV light under applied voltage. Although using two or more additives like a combination of an alignment inducer and RM looks effective in controlling the alignment and stabilization, it causes inhomogeneity in molecular migration onto the surface and takes longer time than using a single additive owing to the complexity in molecular mobility, especially if dimension of substrates were huge.

In this work, we synthesize a special RM that can play both roles of inducing vertical alignment and polymer-stabilizing the pretilt, and that can easily migrate onto the surface with high homogeneity. In the chemical structure, the RM contains three parts: an acrylate functional group as a head, diphenylacetylene as a rigid body, and alkyl chain as a tail. At first, the tail group helps the molecules well mixed with LCs. Second, the body group contributes to building a concrete foundation with raising RM molecules up as they gather on the surface so that a vertical alignment with strong anchoring energy can be induced. Lastly, when the head group begins being polymerized and the RMs become oligomerized, they turn to be unfriendly with LCs due to the structural change from a planar sp^2 to a tetrahedral sp^3 hybridization. This effect brings the RM molecules migrate onto the surface for further polymerization. The molecular motion during polymerization is not complicated because of the monodispersity with a single additive.

Applying voltage during the UV cure process is an efficient way to form pretilt. We divide UV curing process into two steps to achieve it. In step 1, to enhance the uniform movement of the oligomerized RM molecules, migrating onto the surface during the UV irradiation, no voltage is applied, and UV exposure energy is controlled minimally so that the RMs are partially polymerized. In this condition, LC ordering in the vertical alignment is well achieved, which means RMs are quite uniformly moving towards the surface for being polymerized to make monodisperse protrusions. In step 2, voltage is applied to determine the pretilt into domains, and further UV irradiation with sufficient energy completes the polymerization. Therefore, the polymer protrusions are now densely and uniformly generated into the size or shape as it gives the pretilt in the direction of each domain.

2. Materials and methods

2.1. Synthesis of reactive monomer: 4-((4-pentylphenyl)ethynyl) phenyl acrylate

The RM, 4-((4-Pentylphenyl)ethynyl)phenyl acrylate, was synthesized according to a procedure described in the literatures [24,25]. 4-((4-Pentylphenyl)ethynyl)phenol (3.0 g) and triethylamine (3.5 g) were added to 50 ml of tetrahydrofuran (THF), and the mixture was cooled to 5 °C. To this mixture, 1.6 g of acryloyl chloride in 10 ml THF was added dropwise for 5 min. After stirring the reaction mixture for 1 h, 100 ml of ethyl acetate was added, and the organic layer was separated and washed with aq. $NaHCO_3$ and distilled water. The solution was dried with anhydrous sodium sulfate, and the solvent was removed under reduced pressure to obtain 3.1 g of crude product. After purification by column chromatography in silica gel with mixed eluent of ethyl acetate : *n*-hexane (1:8 v/v), 2.1 g of 4-((4-pentylphenyl)ethynyl)phenyl acrylate was obtained (Figure S1). ^{1}H NMR (500 MHz, $CDCl_3$): δ = 0.87–0.91 (t, 3H), 1.28–1.36 (m, 4H), 1.57–1.65 (m, 2H), 2.57–2.63 (t, 2H), 6.00–6.05 (q, 1H), 6.28–6.35 (q, 1H), 6.58–6.64 (q, 1H), 7.10–7.18 (m, 4H), 7.41–7.45 (d, 2H), 7.51–7.55 (d, 2H) ppm. (Figure S2)

2.2. Materials

We used a nematic LC (ZSM-7125, JNC Corporation, T_{NI} = 76.0 °C, Δn = 0.101 at 25 °C, n_e = 1.583, n_o = 1.482, $\Delta\varepsilon$ = -2.90) and synthesized RM (T_{CN} = 59.6 °C, T_{NI} = 67.1 °C) with the concentration in the mixture LC:RM (98.8:1.2). The mixture was well vortexed at the temperature above the isotropic transition temperature.

2.3. Cells

Indium-tin oxide (ITO) was coated on two glass substrates as an electrode and patterned on one of the substrates before sandwiched with the cell gap d = 3.1 μm. The electrode pattern looks a fishbone, and it is four-fold asymmetric with the width and spacing $w = l$ = 3 μm as shown in Fig. 2 (d, e).

2.4. Characterization

Nuclear magnetic resonance (NMR, JNM-ECZ500R, JEOL) and Fourier transform infrared spectrometry (FTIR, Frontier IR, Perkin Elmer) were conducted to identify the chemical structure of the synthesized RM (See Supplemental Information for details). The phase transitions were detected by differential scanning calorimetry (DSC, Q20, TA Instruments). A polarizing optical microscope (POM, Eclipse E600, Nikon) with a charge-coupled device (CCD, DXM 1200, Nikon) was used for observation of optical microimages and conoscopic images of cells. The pretilt angle was measure by a modified crystal rotation method (PAMS, Sesim Photonics Technology) in which the transmittance was measured upon varying the polar angle in the plane, parallel to the applied electric field direction. The electro-optical measurements were done by setting up with a function generator (33521A, Agilent), a photodetector (DET36A/M (350–1100 nm), Thorlabs) and an oscilloscope (DPO 2024B, Tektronix). A square wave was applied to the samples. The response times were determined between the interval of 10% and 90% of the maximum transmittance. In the optic setup, light travels through cells, which are placed in between crossed polarizers, in a way that the optic axis of LC at a voltage-on state is 45° to the polarization directions. The UV spectroscopy was done by a UV–Vis spectrometer (S-3100, Scinco). The surface morphology was evaluated by using an atomic force microscope (AFM, Park NX10, Park systems).

3. Results and discussion

3.1. The role of synthesized reactive mesogen in the pretilt formation

Schematic description of the molecular behavior in fabrication process is illustrated in Fig. 1. The LC director configuration in each stage is discussed with the measurement results in Fig. 2. The chemical structure of the synthesize RM and its schematic description are shown in Fig. 1(a). After injecting the LC-RM mixture into an empty cell, the LCs are vertically aligned although there is minor imperfection (Fig. 1(b)). We believe that this is probably due to the spontaneous migration of some RM molecules onto the surface of glass substrates owing to their relatively polar acryl functional

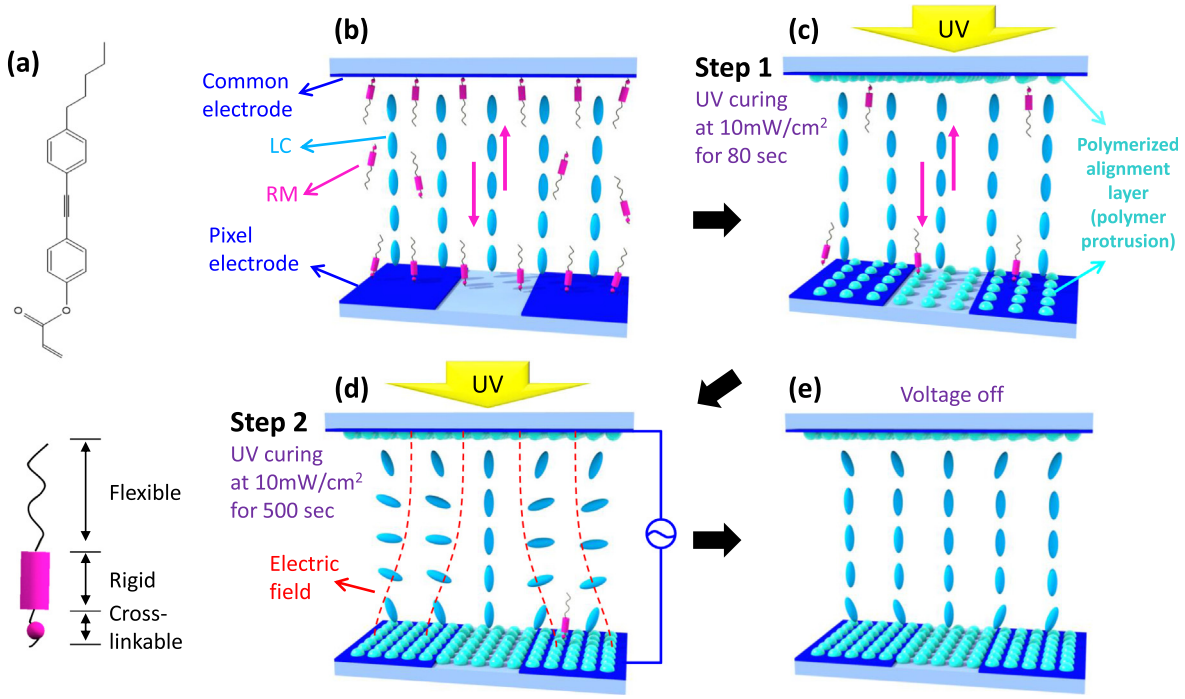

Fig. 1. Schematic description of the molecular behavior in fabrication process. (**a**) Chemical structure of synthesized RM in this work that contains cross-linkable, rigid, and flexible parts. (**b**) After infiltration of LC-RM mixture. (**c**) The first UV exposure that induces the RM partially migrating to the surfaces (step 1). (**d**) Voltage on and the second UV exposure (step 2). (**e**) After voltage off. Two-domain PS-VA achieved by the directed pretilt at the surfaces. We indicate migration of RMs onto the surface by red arrows.

group, which prefers the surface to the bulk LCs. When the RM molecules are located on the surface, their rigid diphenylacetylene body and long alkyl tails could induce the vertical alignment. We conduct curing **step 1**, by irradiating UV at 10 mW/cm2 for 80 sec as shown in Fig. 1(c) to ensure the perfection in its uniformity and the vertical LC alignment. In this step, we modulate the UV energy to be minimal enough for the RMs to migrate onto the surface and partially be cured. In **step 2**, voltage is applied (at operat-

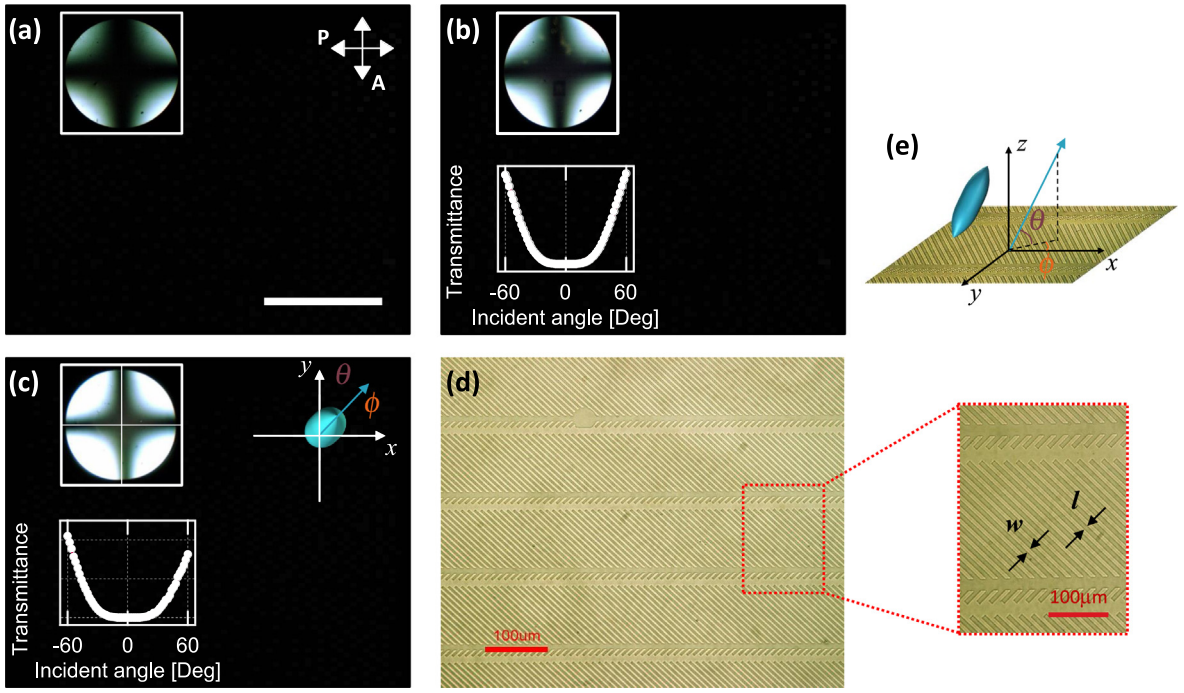

Fig. 2. Polarizing optical microscopy (POM) images corresponding to the fabrication steps in Fig. 1 and the bright field image of the patterned electrodes. (**a**) Vertical alignment after infiltration of LC-RM mixture. (**b**) The state after the first UV exposure (step 1). (**c**) After voltage on and the second UV exposure (step 2). The insets are conoscopic images and measured incident angle-dependent transmittance when conducting a modified crystal rotation method. The schematic inset in (c) describes the director tilt in a polar angle θ and an azimuthal angle ϕ. The scale bar is 200 μm. (**d**) The patterned electrode whose width and space are $w = l = 3$ μm. The scale bar is 100 μm. (**e**) Schematic of the director tilt with respect to the electrode direction in the polar coordinate.

ing voltage V_{op} = 5.2 V) between top and bottom ITO – the patterned electrode on the bottom substrate helps to form the lateral component in the electric field – to reorient LC in a desired initial director configuration (Fig. 1(d)). The LC directors in the middle cell region are well reoriented, perpendicular to the electric field direction, into both polar and azimuthal angles that we aim. The second UV irradiation at 10 mW/cm^2 for 500 sec then complete the polymerization under the applied voltage. In this step, the residual RM molecules are fully polymerized on the surface to secure the LC pretilt that is stabilized after removal of voltage (Fig. 1(e)).

3.2. Verification of vertical alignment and pretilt

In Fig. 2(a-c), we verify the vertical alignment and pretilt corresponding to each fabrication step in Fig. 1 as the POM images show dark states. In addition to the observation of the optical status of the cell, we confirm the vertical alignment with the conoscopy and measure the pretilt angles (insets in Fig. 2(a-c)) formed after the UV cure step 1 and both step 1, 2 via a modified crystal rotation method (see Experimental Section). LC shows vertical alignment after filling into a cell (Fig. 2(a)) and the UV cure step 1 gives no change in overall pretilt angle. The alignment of LC, however, becomes more ordered as the conoscopic image shows brighter light leakage at the four corners (inset in Fig. 2(b)) than before the step 1 (inset in Fig. 2(a)). We further observe that the light leakage in the conoscopic image after UV cure step 1, 2 in Fig. 2 (c) is even brighter than that in Fig. 2(b). This implies that the ordering of LC becomes higher after the UV cure. More importantly, the bright region at the left bottom corner is larger than the right top corner in Fig. 2(c). As the broken symmetry in the four-fold rotational axis of the electrode pattern, four-fold symmetry is not achieved in the conoscopic image, which means the pretilt is formed. To verify it, we measured the pretilt angle via a modified crystal rotation method as shown in the plots in Fig. 2(b,c). The measured pretilt angle after the step 1 is θ_1 = 89.9° and after step1, 2 it is θ_2 = 88.7° at the azimuthal angle $\phi \sim 45°$, which is perpendicular to the longer axis of the patterned electrode as shown in Fig. 2 (d,e). The measured pretilt angle is in a good agreement with the previously reported results [26].

We in addition discuss about the structural effect of the polymerization. Exposing UV on one side of the cell may be treated as an asymmetric external stimulus. We believe there are two different reasons that the RMs migrate on to the surface. At first, the RMs prefer the surface to the bulk LCs because the head part of synthesized RM with an arylate functional group is polar. Secondly, under exposed with low UV intensity, some portion of RM molecules is oligomerized. The generated oligomers may induce LC deformation that causes elastic energy cost. Thus, they would migrate onto the surface to reduce the free energy. From the first reason, RMs have no preferred substrate they want to move. From the second reason, they would be polymerized on the surface but the cell gap (d = 3.2 μm) is not too big for UV reaching the other substrate. Thus, the polymerization may occur with similar rate on both surfaces.

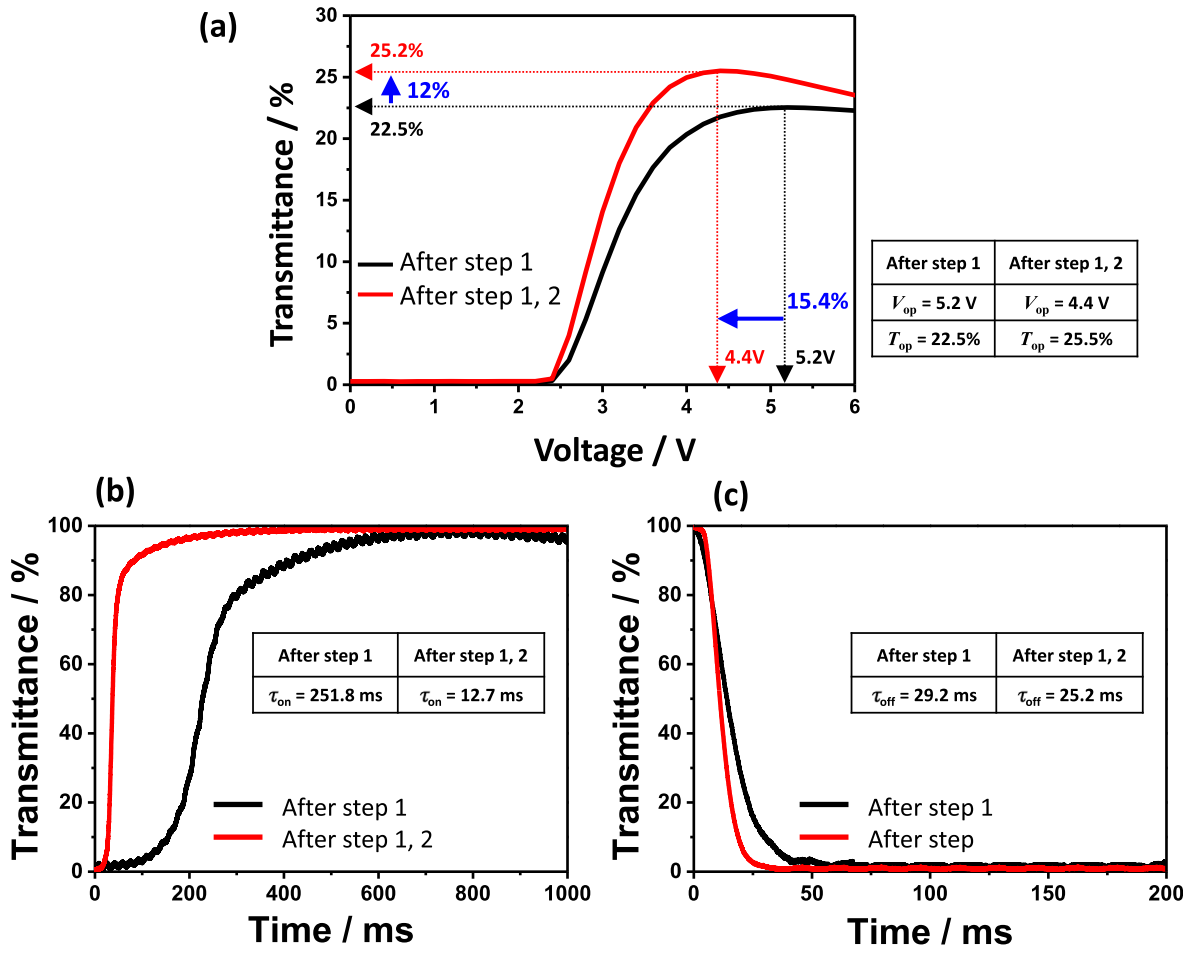

Fig. 3. Electro-optic properties after done with the UV cure step 1 and after both step 1, 2. (a) Voltage-dependent and (b, c) time-dependent transmittance curves that show rising (τ_{on}) and falling (τ_{off}) times.

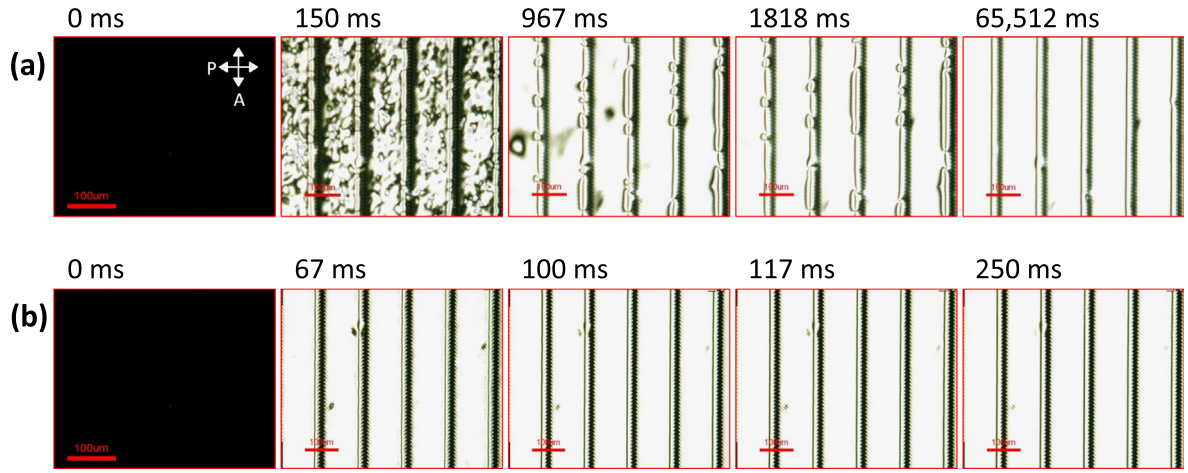

Fig. 4. Time-resolved polarizing optical microscopy (POM) images of the cells under the operating voltage V_{op} = 5.2 V (**a**) after done with the UV cure step 1 and (**b**) after the step 1, 2. Scale bars are 100 μm.

3.3. Enhancement of electro-optic properties

We measure electro-optic properties of the cells after done with the UV cure step 1 and after the UV cure step 1, 2 to analyze the contribution of the pretilt (Fig. 3). The voltage-dependent transmittance (*V-T*) curves show the threshold and operating voltages V_{th} = 2.5 V and V_{op} = 5.2 V after the step 1 as shown in Fig. 3(a). After the step 1, 2, the threshold voltage remains almost unchanged, but the operating voltage is reduced to V_{op} = 4.4 V, which is 15.4% reduced. In addition, the result shows transmittance at the operating voltage is enhanced up to 12%. After the step 1, 2, the fixed pretilt and specified azimuthal angle allow the LC reorientation in a guided direction to reach the maximum transmittance. Without the pretilt, LC reorientation is not guided, and even topological defects may occur, which result in relatively low transmittance.

We also measured the response times to verify how the pretilt of LCs contributes to the LC reorientation and relaxation dynamics. The rising time τ_{on} and falling time τ_{off} after done with the UV cure step 1 (after the UV cure step 1, 2) are τ_{on} = 251.8 (12.7) ms and τ_{off} = 29.2 (25.2) ms respectively as shown in Fig. 3(b, c). Both rising and falling times after the step 1, 2 are shorter than those after the step 1, especially for the rising time. The longer response times are resultant from undirected reorientation of the LCs. Upon the applied voltage, the vertical LC alignment with no pretilt is not able to guide preferential azimuthal direction when LC reorients their optic axis toward into the plane of the surface. The measured result of the falling time after both step 1, 2 also shows quicker response than that in the step 1 although the difference is relatively minor. We believe the anchoring strength upon the case both step 1, 2 are done becomes stronger because the surface roughness and the peak height get higher owing to the bigger polymer protrusion as schematically described in Fig. 1(d,e).

We keep our focus on the reason of the quicker response upon voltage on. We believe the observation of POM images within short time frames should be helpful to understand the behavior of the LC reorientation with the result shown in Fig. 4. The result after done with the UV cure step 1 shows a chaos status of entangled disclinations at *t* = 150 ms in Fig. 4(a) owing to the absence of the pretilt when the operating voltage V_{op} = 5.2 V is applied. It takes long time for the disclinations to be annealed to show clear bright state without any defects. According to the result in Fig. 4(a), some defects still exist near the region above the main bone of the electrode pattern in 1818 ms, and the defects vanish after more than 65000 ms. On the other hand, the case after step 1, 2 are done, the clear bright texture without defect lines is achieved within 67 ms as shown in Fig. 4(b), clearly proving the pretilt is well produced.

3.4. Verification of photopolymerization and surface morphology of polymers

Now we verify how the degree of polymerization can be controlled based on the UV exposure energy onto the RMs. To control the degree of polymerization, quantifying the UV energy with respect to the number of acrylates in the RMs. In Fig. 5, the measured spectrum when no UV exposure (0 J/cm^2) is in excellent agreement with the UV/Vis spectrum of acrylates [27]. The measured spectrum of the cured cell under UV exposure energy dosage higher than 4.8 J/cm^2 no longer shows much difference in the spectral curves, which means no residual RM in the cell is cured above this UV exposure energy. In UV step 1, we control the UV energy at 0.8 J/cm^2 (below 4.8 J/cm^2), which partially polymerize RMs with

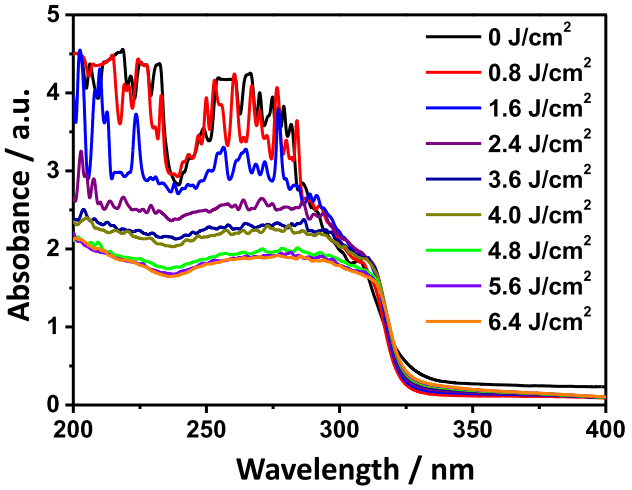

Fig. 5. UV spectra when the acrylates are polymerized by UV curing. The spectral absorbance does not change much when the UV cure with exposure energy above 4.8 J/cm^2.

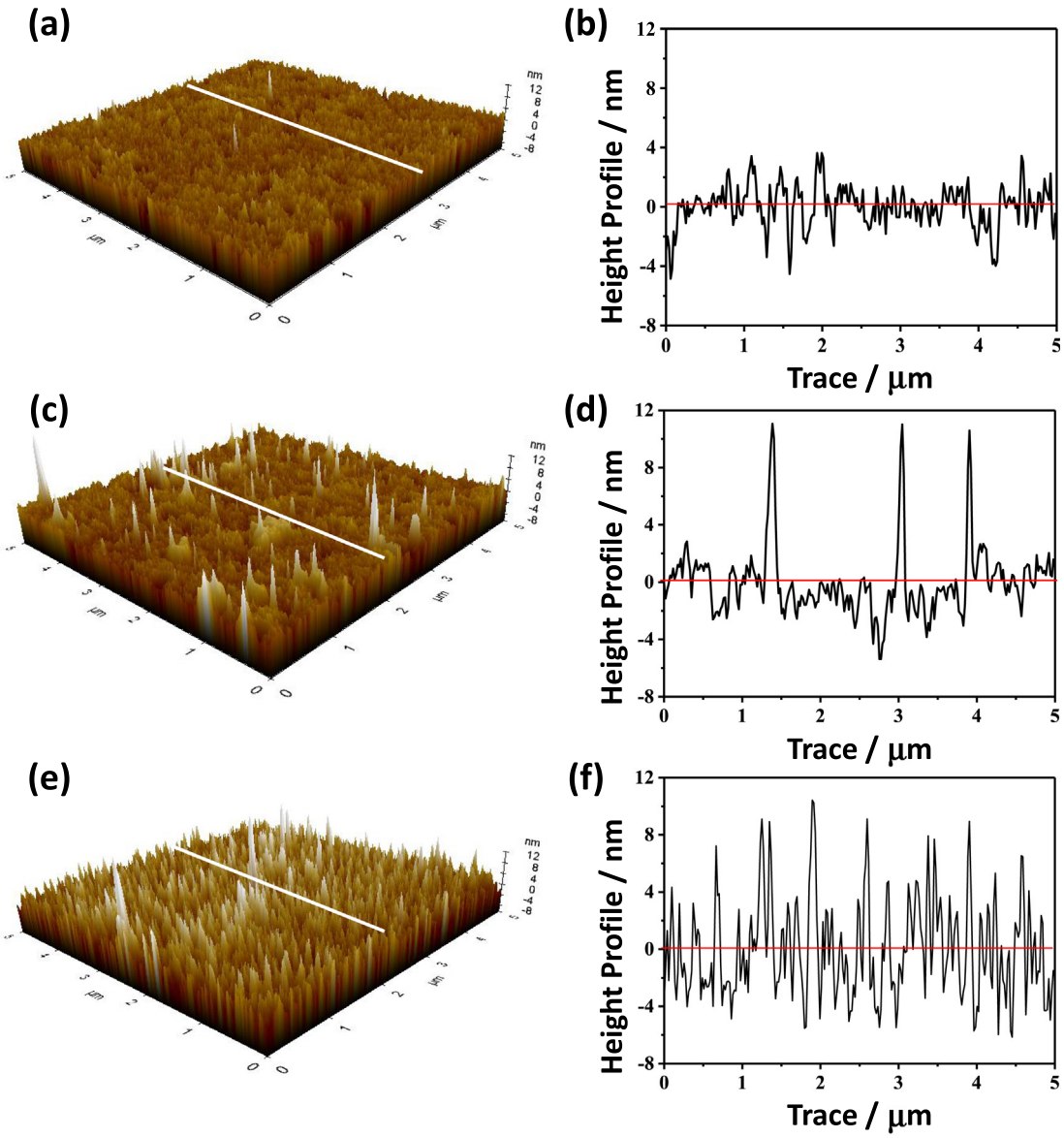

Fig. 6. Atomic force microscopy (AFM) analysis of surface topography of (**a,b**) bare ITO electrode on a substrate, (**c,d**) after done with the UV cure step 1 and (**e,f**) after the step 1, 2. (a,c,e) 2D and (b,d,f) 1D surface profile.

no induction of pretilt. In UV step 2, the UV energy is controlled at 5 J/cm^2 to polymerize all RMs.

Finally, we visualize the surface morphology after the UV curing steps by AFM measurement (Fig. 6). The topographic AFM images and corresponding height profiles help us to directly confirm the degree of polymerization at the surface as we expect. In the result with a bare ITO glass, the protruded height does not exceed 4 nm as shown in Fig. 6(a, b). The cell after done with the step 1 shows relatively higher density of protrusion with the height above 4 nm and some peaks reach above 8 nm. The density is measured by approximately 0.6 μm^{-1} as shown in Fig. 6(c,d) In case of the cell after done with both step 1, 2, on the other hand, the density of protrusion with the height above 4 nm becomes 2.4 μm^{-1} and much more numbers of peaks reach above 8 nm as shown in Fig. 6(e,f). These results clearly verify and confirm the polymer protrusion on the surface is well and densely built after the UV step 1,2, which significantly contributes to the enhancement of the electro-optic properties of the cell with well-achieved pretilt.

4. Conclusion

In this work, we propose a binary mixture consisting of a liquid crystal (LC) and a synthesized reactive mesogen (RM). The RM specially plays two roles of a vertical alignment inducer and a polymer-stabilizer. In this way, conventional polyimide layer, which has been the most reliable material to produce the alignment but requires high-thermal process, is unnecessary and only one additive is mixed with the host LC to produce vertical alignment. In addition, we propose two-step UV curing process to control the pretilt. In UV cure step 1, we modulate the degree of polymerization by controlling UV energy such that the polymer-stabilization is partially done to induce the uniform vertical alignment. In UV cure step 2, we apply voltage through a patterned electrode to form the pretilt in the vertical alignment. Further UV exposure then complete the polymerization of RMs to hold the pretilt tight and to secure the higher order in the alignment.

The proposed method shows four-improved approaches: 1) the LC-RM binary mixture used in this work gives successful vertical

alignment at the ground state; 2) varying UV exposure energy in each step enables us to control the degree of polymerization of RM at the surface; 3) the UV cure step 1 enhances the ordering of LC vertical alignment; 4) the result after the UV cure step 1, 2 well achieves the pretilt in the domains of designated patterned electrodes. The demonstrated polymer-stabilized vertical alignment (PS-VA) mode cell exhibits excellent electro-optic properties, such as quick response times, reduced threshold and operating voltages, and high on-state transmittance. In addition, this method requires LC and RM, only two materials in the mixture with no additional material for the vertical alignment and significantly reduces the fabrication processing steps compared to those conventional methods to achieve the pretilt. We believe this method will not only enhance the engineering in PS-VA modes but also contribute to explore the scientific interests in the field of surface alignment controlling techniques.

CRediT authorship contribution statement

Young Jin Lim: Methodology, Writing – original draft. **Jun Hyeok Lee:** Validation, Investigation, Data curation. **Gwan Yong Lee:** Validation, Investigation. **Mira Jo:** Investigation. **Eun Ji Kim:** Investigation. **Tae Hyung Kim:** Investigation. **MinSu Kim:** Methodology, Formal analysis, Writing – original draft, Writing – review & editing, Supervision, Funding acquisition. **Myong-Hoon Lee:** Resources, Writing – review & editing. **Seung Hee Lee:** Conceptualization, Writing – review & editing, Supervision, Funding acquisition.

Declaration of Competing Interest

The authors declare that they have no known competing financial interests or personal relationships that could have appeared to influence the work reported in this paper.

Acknowledgements

This work was supported by the Basic Science Research Program through the National Research Foundation of Korea (NRF) funded by the Ministry of Education (2016R1D1A1B01007189) and (2020R1A6A3A01100570), and by the Innovation Lab support program for material, parts, equipment (20016808) funded by the Ministry of Trade, Industry & Energy (MOTIE, Korea)

Appendix A. Supplementary material

Supplementary data to this article can be found online at https://doi.org/10.1016/j.molliq.2021.117302.

References

[1] A. Takeda, S. Kataoka, T. Sasaki, H. Chida, H. Tsuda, K. Ohmuro, T. Sasabayashi, Y. Koike, K. Okamoto, 41.1: A Super-High Image Quality Multi-Domain Vertical Alignment LCD by New Rubbing-Less Technology, SID Symp, Dig. Tech. Pap. 29 (1) (1998) 1077, https://doi.org/10.1889/1.1833672.

[2] S.W. Park, S.H. Lim, Y.E. Choi, K.-U. Jeong, M.-H. Lee, H.S. Chang, H.S. Kim, S.H. Lee, Multi-domain vertical alignment liquid crystal displays with ink-jet printed protrusions, Liq. Cryst. 39 (4) (2012) 501–507, https://doi.org/10.1080/02678292.2012.657697.

[3] Y. Taniguchi, H. Inoue, M. Sawasaki, Y. Tanaka, T. Hasegawa, T. Sasaki, Y. Koike, K. Okamoto, 25.3: An Ultra-High-Quality MVA-LCD Using a New Multi-Layer CF Resin Spacer and Black-Matrix, SID Symp, Dig. Tech. Pap. 31 (1) (2000) 378–381, https://doi.org/10.1889/1.1832961.

[4] K. Hanaoka, Y. Nakanishi, Y. Inoue, S. Tanuma, Y. Koike, K. Okamoto, 40.1: A New MVA-LCD by Polymer Sustained Alignment Technology, SID Symp, Dig. Tech. Pap. 35 (1) (2004) 1200, https://doi.org/10.1889/1.1821335.

[5] S.G. Kim, S.M. Kim, Y.S. Kim, H.K. Lee, S.H. Lee, G.-D. Lee, J.-J. Lyu, K.H. Kim, Stabilization of the liquid crystal director in the patterned vertical alignment mode through formation of pretilt angle by reactive mesogen, Appl. Phys. Lett. 90 (26) (2007) 261910, https://doi.org/10.1063/1.2752105.

[6] Y.R. Kwon, Y.E. Choi, P. Wen, B.H. Lee, J.C. Kim, M.-H. Lee, K.-U. Jeong, S.H. Lee, Polymer stabilized vertical alignment liquid crystal display: Effect of monomer structures and their stabilizing characteristics, J. Phys. D. Appl. Phys. 49 (16) (2016) 165501, https://doi.org/10.1088/0022-3727/49/16/165501.

[7] J.M. Geary, J.W. Goodby, A.R. Kmetz, J.S. Patel, The mechanism of polymer alignment of liquid-crystal materials, J. Appl. Phys. 62 (10) (1987) 4100–4108, https://doi.org/10.1063/1.339124.

[8] J. Hoogboom, T. Rasing, A.E. Rowan, R.J.M. Nolte, LCD alignment layers. Controlling nematic domain properties, J. Mater. Chem. 16 (14) (2006) 1305–1314, https://doi.org/10.1039/B510579J.

[9] M. Jiao, Z. Ge, Q. Song, S.-T. Wu, Alignment layer effects on thin liquid crystal cells, Appl. Phys. Lett. 92 (6) (2008) 061102, https://doi.org/10.1063/1.2841642.

[10] Y.J. Lim, J.H. Yoon, H. Yoo, S.M. Song, R. Manda, S. Pagidi, M.-H. Lee, J.-M. Myoung, S.H. Lee, Fast switchable field-induced optical birefringence in highly transparent polymer-liquid crystal composite, Opt. Mater. Express. 8 (12) (2018) 3698, https://doi.org/10.1364/OME.8.003698.

[11] M.S. Kim, L.-C. Chien, Topology-mediated electro-optical behaviour of a wide-temperature liquid crystalline amorphous blue phase, Soft Matter 11 (40) (2015) 8013–8018, https://doi.org/10.1039/C5SM01918D.

[12] R. Manda, S. Pagidi, Y. Heo, Y.J. Lim, M.S. Kim, S.H. Lee, Electrically tunable photonic band gap structure in monodomain blue-phase liquid crystals, NPG Asia Mater. 12 (2020) 1–9, https://doi.org/10.1038/s41427-020-0225-8.

[13] S. Pagidi, R. Manda, H.S. Shin, J. Lee, Y.J. Lim, M.S. Kim, S.H. Lee, Enhanced electro-optic characteristics of polymer-dispersed nano-sized liquid crystal droplets utilizing PEDOT:PSS polymer composite, J. Mol. Liq. 322 (2021) 114959, https://doi.org/10.1016/j.molliq.2020.114959.

[14] S.-C. Jeng, C.-W. Kuo, H.-L. Wang, C.-C. Liao, Nanoparticles-induced vertical alignment in liquid crystal cell, Appl. Phys. Lett. 91 (6) (2007) 061112, https://doi.org/10.1063/1.2768309.

[15] Y. Wang, C. Xu, A. Kanazawa, T. Shiono, T. Ikeda, Y. Matsuki, Y. Takeuchi, Thermal stability of alignment of a nematic liquid crystal induced by polyimides exposed to linearly polarized light, Liq. Cryst. 28 (3) (2001) 473–475, https://doi.org/10.1080/02678290010017962.

[16] R. He, P. Wen, S.-W. Kang, S.H. Lee, M.-H. Lee, Polyimide-free homogeneous photoalignment induced by polymerisable liquid crystal containing cinnamate moiety, Liq. Cryst. 45 (9) (2018) 1342–1352, https://doi.org/10.1080/02678292.2018.1441459.

[17] S.-H. Lee, J.-H. Son, W.-C. Zin, S.H. Lee, J.-K. Song, Self-constructed stable liquid crystal alignment in a monomer-liquid crystal mixture system, Liq. Cryst. 39 (9) (2012) 1049–1053, https://doi.org/10.1080/02678292.2012.693630.

[18] H. Qi, T. Hegmann, Formation of periodic stripe patterns in nematic liquid crystals doped with functionalized gold nanoparticles, J. Mater. Chem. 16 (2006) 4197–4205, https://doi.org/10.1039/b611501b.

[19] W.-Y. Teng, S.-C. Jeng, C.-W. Kuo, Y.-R. Lin, C.-C. Liao, W.-K. Chin, Nanoparticles-doped guest-host liquid crystal displays, Opt. Lett. 33 (15) (2008) 1663, https://doi.org/10.1364/OL.33.001663.

[20] C.-Y. Ho, J.-Y. Lee, Fabrication of pseudo-pi vertical alignment mode liquid crystal devices with ultra-violet polymerisation and investigations of their electro-optical characteristics, Liq. Cryst. 37 (8) (2010) 997–1012, https://doi.org/10.1080/02678291003746247.

[21] Y. Inoue, M. Gushiken, G. Sudo, S. Kosaka, M. Hayashi, K. Shimizu, M. Takachi, 83–3L: Late-News Paper : A Novel High Reactive and High Reliable Monomer for Polymer-Sustained Alignment Liquid Crystal Displays, SID Symp. Dig. Tech. Pap. 48 (2017) 712–715, https://doi.org/10.1002/sdtp.11742.

[22] Q. Li, Y. Zhang, H. Wei, W. Cui, T.J. Tseng, C.C. Hsieh, C.Y. Chiu, Study on the effect of controlling the pretitle angle using RM with multipolymerizable functional group, in: Dig. Tech. Pap. - SID Int. Symp., Blackwell Publishing Ltd, 2019: pp. 371–374. https://doi.org/10.1002/sdtp.12934.

[23] I. Son, C. Kim, J.H. Kim, B. Lee, J.Y. Yoo, J.H. Lee, Fabrication of a new homeotropic alignment layer for nematic liquid crystals using an in situ self-assembly of alkylated benzoic acid derivative, Mol. Cryst. Liq. Cryst. 644 (1) (2017) 98–102, https://doi.org/10.1080/15421406.2016.1277460.

[24] H. Hasebe, K. Takeuchi, H. Takatsu, Acrylate compound and liquid crystal device produced by using the compound, JPH0717910A, 1995.

[25] H. Hasebe, K. Takeuchi, H. Takatsu, Properties and application of UV-curable liquid crystals, J. Photopolym. Sci. Technol. 10 (1) (1997) 25–30, https://doi.org/10.2494/photopolymer.10.25.

[26] L. Weng, P.-C. Liao, C.-C. Lin, T.-L. Ting, W.-H. Hsu, J.-J. Su, L.-C. Chien, Anchoring energy enhancement and pretilt angle control of liquid crystal alignment on polymerized surfaces, AIP Adv. 5 (9) (2015) 097218, https://doi.org/10.1063/1.4932153.

[27] X.-S. Chai, F.J. Schork, E.M. Oliver, ATR-UV monitoring of methyl methacrylate miniemulsion polymerization for determination of monomer conversion, J. Appl. Polym. Sci. 99 (4) (2006) 1471–1475, https://doi.org/10.1002/app.22658.